Infrared Absorption in Gallium Arsenide-Gallium Phosphide Alloys

OSAMURA, Kozo; MURAKAMI, Yotaro

OSAMURA, Kozo ...[et al]. Infrared Absorption in Gallium Arsenide-Gallium Phosphide Alloys. Memoirs of the Faculty of Engineering, Kyoto University 1970, 32(3): 361-377

Infrared Absorption in Gallium Arsenide-Gallium Phosphide Alloys*

By

Kozo OSAMURA and Yotaro MURAKAMI**

(Received March 31, 1970)

The infrared absorption has been quantitatively investigated with respect to the shape, the temperature dependence and the carrier concentration dependence of the additional absorption band in the region from 1000 to 4000 cm^{-1}.

The experimental method for the determination of the threshold energy was discussed. The present experimental results have given a reasonably clear indication of the difference between the additional absorptions in *n*-GaAs-rich alloys and ones in *n*-GaP-rich alloys. Especially, the additional bands in *n*-GaAs-rich alloys were concluded to occur by a transition of conduction electron from the lowest band minimum to the upper subsidiary one. The dependence of the threshold energy on composition x was found to be expressed as $E_t=0.29-0.67x$ (eV). The empirical cross over point occurred at 43 mol% GaP.

On the other hand, in *n*-GaP and GaP-rich alloys, the additional band showed a relatively sharp peak and all the absorption shapes were similar to the previous analysis. The threshold energy was found to depend to a small extent on the composition. The dependence could be illustrated in terms of the composition dependence of the ionization energy.

1. Introduction

Recently, studies on the optical properties of semiconductors have been developed, mainly in the region from visible rays to infrared ones, where it is possible to obtain much information about details of electronic energy band structure, impurity levels in the forbidden band, conduction electrons and lattice vibration of crystal.

In several III-V semiconductors, there is present such a band that has a subsidary minimum above a few tenth of eV from the bottom of the lowest conduction band[1]. The exploration of secondary conduction-band minima has attracted considerable interest for two reasons. Firstly such minima can be important for high-field transport properties, and secondly, an experimental determination of their position in energy and $\boldsymbol{k}$ space is valuable in comparison with

---

[*] The preliminary report was published in J. Phy. Soc. Japan 26 (1969) 1083.

[**] Department of Metallurgy

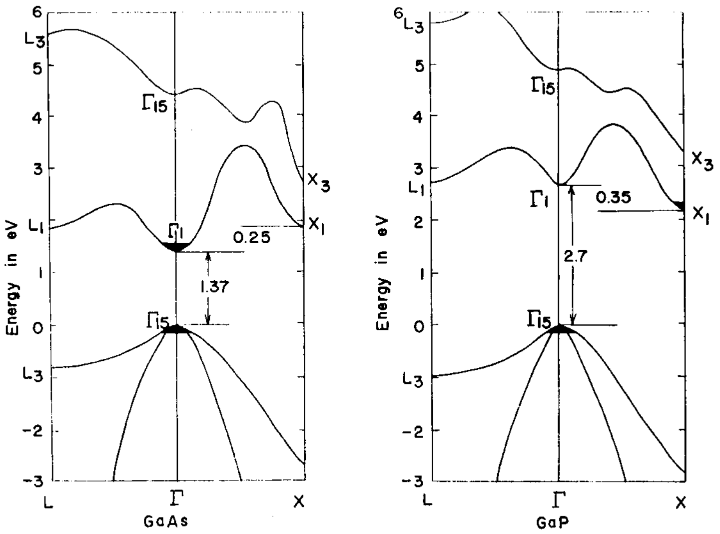

Fig. 1. Conduction band structures of GaAs and GaP.

band calculations. For example, the conduction band structures of GaAs and GaP illustrated in *Figure* 1. The conduction band in GaAs is characterized by a lowest minimum at $k=0$ and by sets of equivalent minimum at X and L of the zone boundary. Such material is called a direct type of semiconductors. Different types of band calculations2)-4) indicate that these secondary minima occur at 0.2—0.6 eV above the primary minimum. A separation of 0.36 to 0.38 eV between primary and lowest secondary minimum has been drived from transport measurements,5)-7) whereas infrared mesurements by Spitzer and Whelan8) were interpreted by Haga and Kimura9) to give a separation of 0.44 eV, and also Balslev 12) reported that the secondary minimum is located at the Brillouin-zone edge along $\langle 100 \rangle$ direction, 0.43 eV above the $k=0$ minimum at 80°K. The influence of uniaxial stress on Gunn effect10) and some properties of GaAs-GaP alloys, e.g., Gunn effect and optical absorption edge,11) have established that the lowest secondary minimum is located at X, the optical studies indicating a separation of 0.4 eV. It is further known that a set of valleys with symmetry X_3 have extremum energies of 0.33 eV above the lower X_1 minima.2) On the other hand, the conduction band in GaP is characterized by a lowest minimum at X and by sets of equivalent minimum at Γ and L as shown in *Figure* 1, where its material is called an indirect type of semiconductor. The energy differences between Γ_1 and X_1 points are experimentally determined to be 0.35—0.4 eV. A set of valleys with symmetry X_3 have extemum energies of 0.3 eV above the lowest minimum X_1.13) Optical transitions between these bands are allowed, and an additional absorption band has been experimentally observed in a short wavelength side of the curves of the intra-band free carrier absorption. It is reported that the bands observed in GaAs[8] and GaSb[14] are due to the inter-conduction band transition.

On the other hand, in such a range of photon energy, an additional absorption arises from the transitions of a donor-electron to the upper conduction band, in which the position of the minimum is the same as that of the minimum of the lowest band. Allen and Hodby have proposed a model to interpret the temperature dependence of the additional absorption in n-GaP and n-GaAs-GaP alloys.[15]

The purpose of the present paper is to investigate quantitatively the shape, the temperature dependence and carrier concentration dependence of the absorption coefficient in n-type GaAs, GaP and GaAs-GaP alloys. A number of explanations have been proposed for this additional absorption. In the following section, some experimental results will be described which give a reasonably clear indication of the difference between the additional absorptions in n-GaAs-rich side alloys and ones in n-GaP-rich alloys.

2. Experimental

Specimens of n-GaAs-GaP alloys for the present work were prepared by the two temperatures method. Polycrystalline ingots were grown from melts with various compositions. A slice of specimen was cut from the top portion of the ingot, where composition was found to be fairly uniform. As to GaAs, the large single crystals were obtained by the present method and, Cr, Se and Te doping in the melt was used for some ingots to have various electron concentrations. The homogeneity of specimens was tested by powder X-ray diffractometer and also by Hall measurements for the determination of conductivity type. The alloy compositions of the samples used in the infrared measurement are given in *Table* 1, where A 1 is a nondoped GaAs crystal with carrier concentration of 1.8×10^{17} cm^{-3}, and A2, A3 are Te doped crystals, and A4 is Se doped one, whose carrier

Table 1. Alloy compositions of the samples.

Sample Number	A1	A2	A3	A4	M1	M2	M3	M4	M5	M6	M7	M10	M11	M12	M15	P1	P2
Mol% GaP	0	0	0	0	4.0	5.0	12.0	12.8	14.7	18.7	22.0	99.0	48.0	50.0	71.0	100	100

concentrations are 3.0×10^{17}, 7.4×10^{17} and 1.0×10^{18} cm^{-3}, respectively, and also P2 is the Cr doped one with high resistivity.

Infrared transmission measurements have been made between 400–4,000 cm^{-1} with Hitachi EP1–G2 spectrometer. The data obtained was for three temperatures of 90, 297 and 423°K. At low temperature the sample was mounted on a cold finger in vacuum. A cryostat vacuum lower than 10^{-4} mmHg was necessary to prevent a build up of ice on the surface of specimen. KBr crystals were used for the windows. The absorption coefficient α was derived from

$$T=\frac{(1-R)^2e^{-\alpha d}}{1-R^2e^{-2\alpha d}}, \tag{1}$$

where R is the bulk reflectance and d is the thickness of a specimen. The reflectance for GaAs and GaP is taken from the table of optical constants by Serphin and Bennett[17] as shown in *Table* 2, where the values for GaAs measured in the present work are in good agreement with their value. The reflectance for the alloy of GaAs-GaP is determined by the interpolation from the values of GaAs and GaP, assuming the linear relation of the dielectric constant.[18] The difference in values is not large, for example, at 2500 cm^{-1} the refractive index of GaAs is 3.30 and that of GaP is 2.95, and so this interpolation does not introduce much error.

Table 2. Reflectance R of gallium phosphide and gallium arsenide as a function of wave number k.

GaP*		GaAs*		GaAs**	
k (cm^{-1})	R	k (cm^{-1})	R	k (cm^{-1})	R
4840	0.244	5000	0.289	5000	0.285
3227	0.244	5333	0.289	4000	0.285
1613	0.243	2500	0.289	3000	0.285
759	0.228	2000	0.289	2000	0.285
714	0.226	1666	0.288	8000	0.285
625	0.220	1428	0.289	1600	0.285
		1250	0.287	1400	0.284
		1111	0.288	1200	0.284
		1000	0.287	1000	0.283
		909	0.287	900	0.278
		833	0.286	800	0.274
				700	0.274

* Seraphin and Bennett[17]
** present work

The curves in *Fig.* 2 give the wave number-dependence of the room temperature

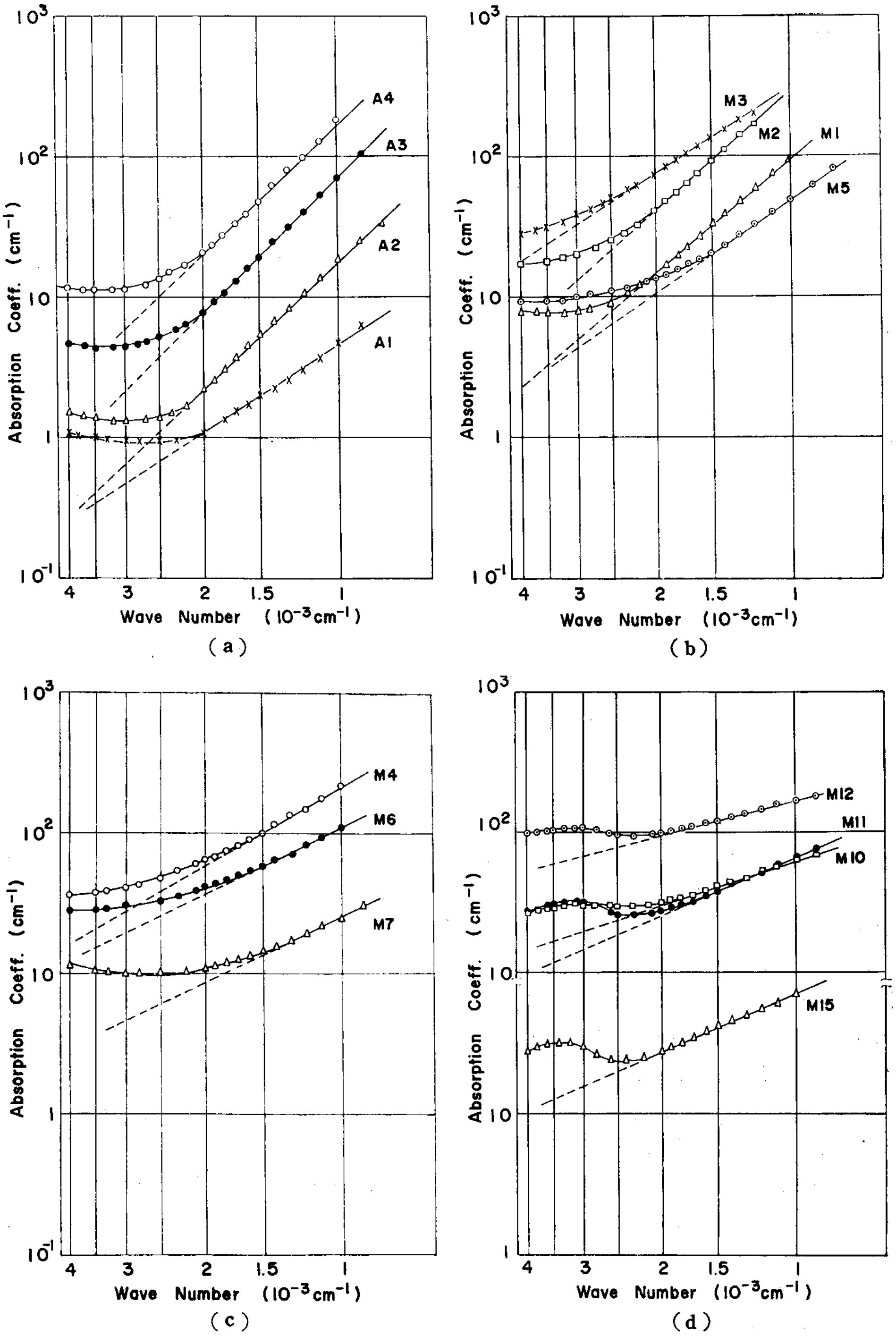

(a)

(b)

(c)

(d)

Fig. 2. Wave number dependence of the room temperature absorption coefficient.
(a) for specimens of A1, A2, A3 and A4.
(b) for pecimenss of M1, M2, M3 and M5.
(c) for specimens of M4, M6 and M7.
(d) for specimens of M10, M12, M11 and M15.

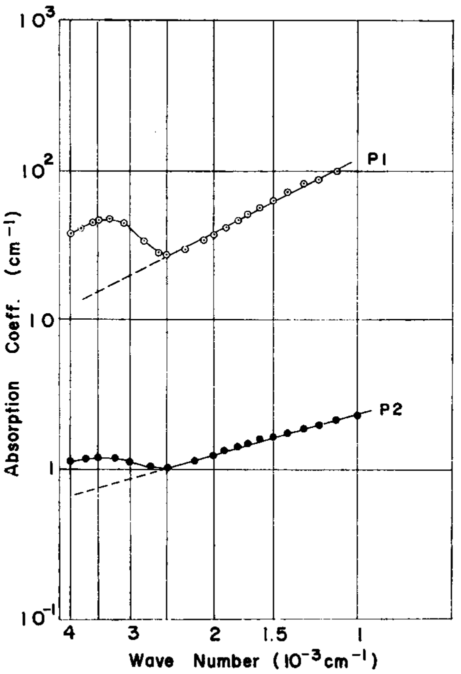

Fig. 2. (e) for specimens of P1 and P2.

absorption coefficient for n-type materials. The absorption at wave numbers <2500 cm^{-1} increases with wave number and with the free-carrier concentration. The absorption at smaller wave numbers is typical of normal free carrier absorption observed in many semiconductors,[21] and the absorption is represented by a symbol α_f, in the present paper. The detail of free-carrier absorption will be discussed in our next paper. The 2000–4000 absorption band also increases with the electron concentration. This phenomenon does not occur in p-type material, but in all n-type-GaAs, -GaP and -GaAs-GaP alloys. The latter absorption band is called as an additional absorption, which is represented as $\Delta\alpha$, in this paper. Then the additional absorption is defined by the following equation,

$$\Delta\alpha = \alpha_{\mathrm{obs.}} - \alpha_f . \qquad (2)$$

When the absorption coefficient is plotted logarithmically as a function of wave number, the free carrier absorption in the smaller wave number region can be well represented by a straight line. The additional absorption could be obtained by extrapolation of the absorption coefficient to the large wave numbers. As to this point, the authors have paid much attention to the derivation of the additional absorption, although the previous workers derived ones from a simple background absorption. The free carrier absorption is proportional to the minus xth power of wave number k. It has been precisely determined that x is 3.0 in n-GaAs with high carrier concentration and is 2.5 in n-GaAs with low carrier concentration. In GaP, x is experimentally determined to be 1.5.

The measured additional absorption spectra between 1000 and 4000 cm^{-1} for n-GaAs samples with various carrier concentrations are shown in Figure 3. It has been observed that the absorption increases with the carrier concentration, but the threshold energy remains unchanged. The spectra for n-GaAs rich alloys are shown in Figure 4. Remarkable changes of the threshold energy have been observed to occur for the specimens with different compositions. On the other

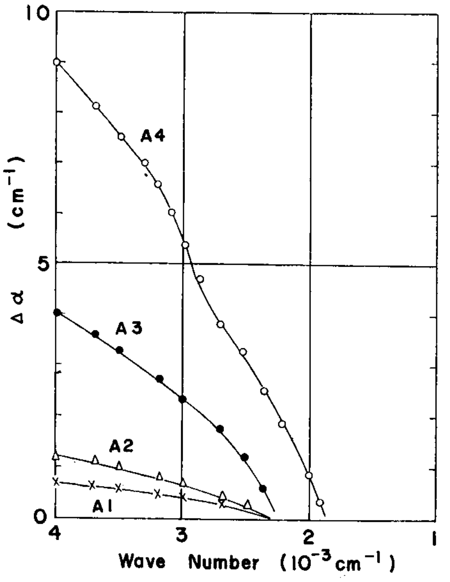

Fig. 3. Additional absorption coefficient as a function of wave number for *n*-GaAs.

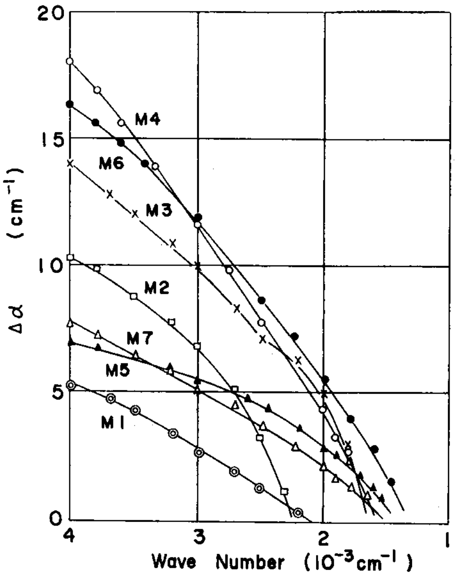

Fig. 4. Additional absorption coefficient as a function of wave number for *n*-GaAs-rich alloys.

hand, a typical spectrum for *n*-GaP sample and the spectra for *n*-GaP rich alloys are shown respectively in Figures 5 and 6, where these spectra are found to have relatively sharp peaks and not to have a composition dependence of the threshold energy. Moreover, the temperature dependence of the additional absorption bands are shown for some typical specimens in Figures 7–10. The features in these alloys could be divided into the following two different groups. The one is the group of *n*-GaP and *n*-GaP rich alloys, whose additional bands have the relatively sharp

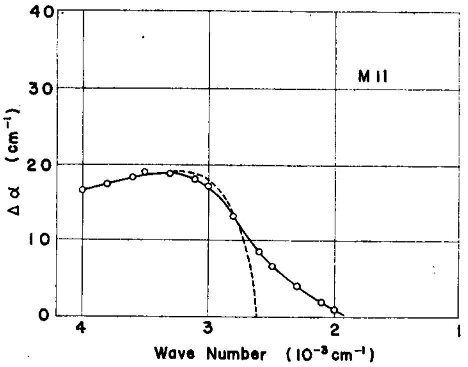

Fig. 5. Additional absorption coefficient as a function of wave number where the dotted curve is obtained by calculation for *n*-GaP-rich alloys. (a) for specimen M11.

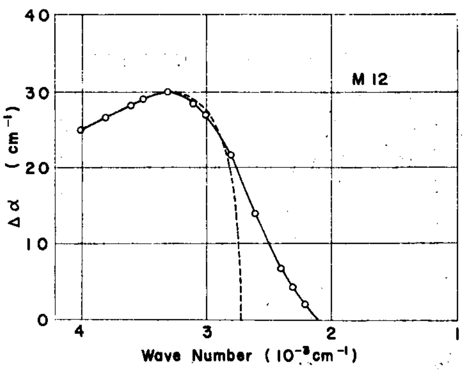

Fig. 5. (b) for specimen M12.

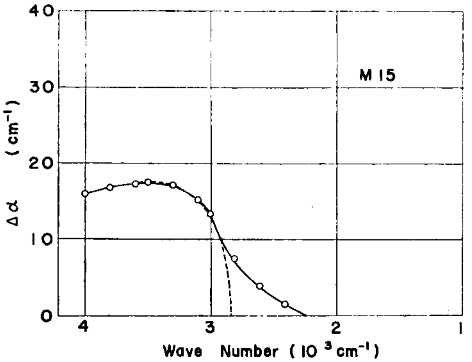

Fig. 5. (c) for specimen M15.

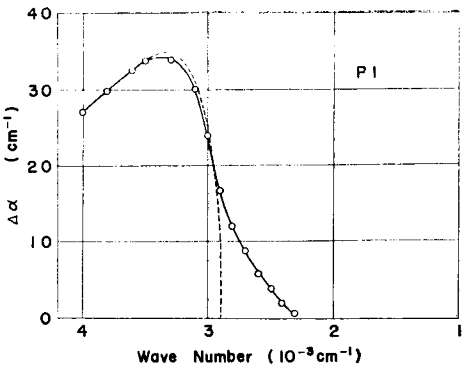

Fig. 6. Additional absorption coefficient as a function of wave number for n-GaP, where the dotted curve is obtained by calculation.

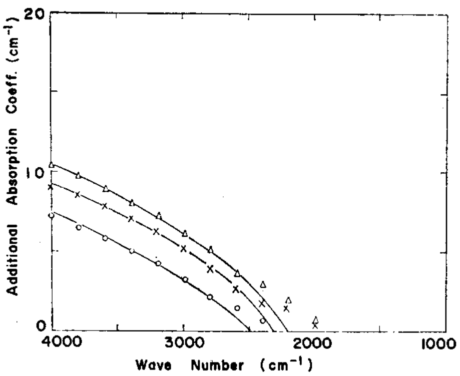

Fig. 7. The additional absorption band for n-GaAs for three different temperatures. Here, -○-, -×- and -Δ- show the data at 90, 297 and about 423°K, respectively.

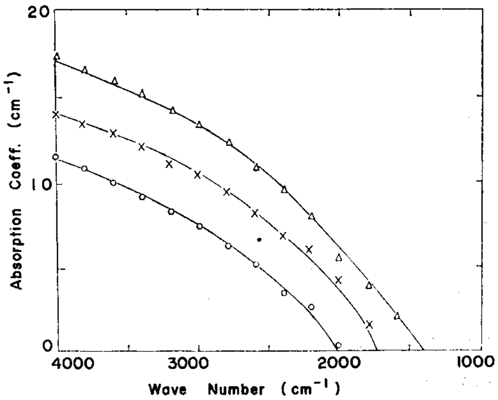

Fig. 8. The additional absorption band for an alloy with 12 mol% GaP for three different temperatures. Here, -○-, -×- and -Δ- show the data at 90, 297 and about 423°K, retpectively.

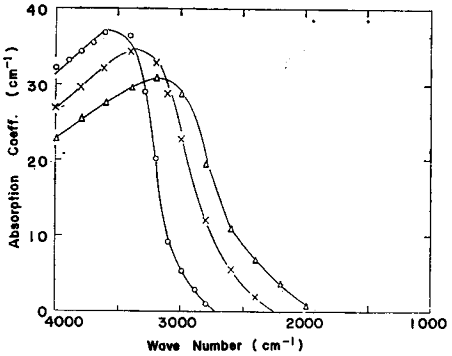

Fig. 9. The additional absorption band for n-GaP for three temperatures. Here, -○-, -×- and -Δ- show the data at 90, 297 and about 423°K, respectively.

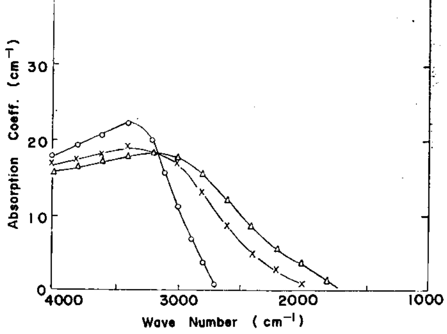

Fig. 10. The additional absorption band for an alloy with 50 mol% GaP for three temperatures. Here, -○-, -×- and -Δ- show the data at 90, 297 and about 423°K, respectively.

peak and similar shapes to Allen and Hodby's results. According to their model, the additional absorption arises from the transition of a donor electron to the upper conduction band in *n*-GaP and *n*-GaP-rich alloys. However, the other group of absorption bands of *n*-GaAs and *n*-GaAs-rich alloys shows the rather broad band, which does not seem to have any remarkable peak. Recently, the additional absorption band in *n*-GaAs has been observed on the short wavelength side of the curves of the intra-band free carrier absorption by several workers[12,9,8)].

The absorption threshold energy was found by fitting the functions discussed below to the experimental curves. The variation with composition is shown in Figure 11. The result for the composition dependence of the absorption threshold seems to give more definite evidence to the difference between the additional absorptions in GaAs-rich side and ones in GaP-rich side.

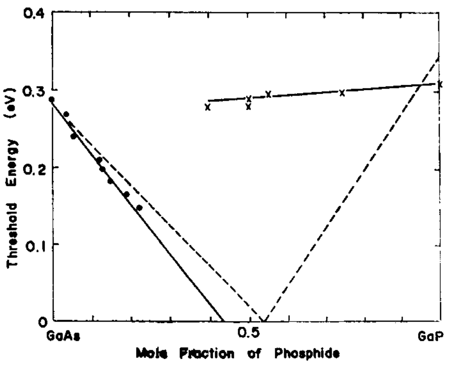

Fig. 11. Emprical threshold energy as a function of alloy compositions.

3. Results and Discussion

3.1 A transition from a shallow donor level to the upper conduction band minimum

As shown in Fig. 1, the lowest conduction band minimum of GaP is in the $\langle 001 \rangle$ direction of $\boldsymbol{k}$ space and is split. There is a subsidiary minimum at $\boldsymbol{k}=0$, and the material contains a variety of impurities of which the important ones for this discussion are hydrogen-like donors near the conduction band minimum and a deep level.

It is reasonable to consider the origin of the absorption for *n*-GaP and GaP-rich alloys as follows; the wave function of a donor level can, to a good approximation, be expanded in terms of wave functions of the conduction band with $\boldsymbol{k}$ values near the conduction band minimum, the spread of $\boldsymbol{k}$ values being independent for tempereture. A direct transition from such a level to an upper conduction band will therefore give an absorption whose width is independent of temperature and whose magnitude is not greatly influenced by temperature.

A simplified treatment of this transition is illustrated by Allen and Hodby.[15] According to their treatment, the additional absorption coefficient due to this process is

$$\Delta\alpha = \frac{Bn_I}{h\nu}\frac{y^{1/2}}{(1+y)^4}, \tag{3}$$

where

$$y \equiv \frac{m_2^*}{m_1^*}\frac{h\nu - E_0 - E_I}{E_I}, \tag{4}$$

B is a constant, n_I is the concentration of electrons in donor levels, m_1^* and m_2^* are scalar effective masses of two conduction band minima, E_0 is the extremum energy from the lowest conduction band minima to the upper band minima, E_I is the donor ionization energy, and $h\nu$ is the photon energy.

The following method is very convenient for fitting the theoretical equation (3) to the experimental curve. The variable z, which is the additional absorption coefficient multiplied by photon energy, is a function of y as shown by the following equation

$$z \equiv \Delta\alpha \cdot h\nu = Bn_I \frac{y^{1/2}}{(1+y)^4} \tag{5}$$

The maximum value of photon energy $h\nu_m$ and z_m are represented as follows,

$$\frac{m_2^*}{m_1^*}\frac{h\nu_m - E_0 - E_I}{E_I} = 1/7 \tag{6}$$

$$z_m = 0.2216\, Bn_I \tag{7}$$

where subscript m refers to the maximum point. A plot of z/z_m vs. y shown in Figure 12 is used in the present analysis. From a plot z vs. $h\nu$ for the experimental data, the values of $h\nu_m$, $h\nu_t$ and z_m are computed easily by using the above relation. Here, $h\nu_t$ is the threshold energy. Thereafter, a reasonable fit is obtained with equation (3), mainly in the large wave number region, where there is an exponential tail as shown by the solid curves in Figures 5 and 6. Some parameters obtained from the curve fitting are also shown in Table 3. There appears to be a good agreement between experimental values and the calculated ones from the assumption that the additional absorption band in GaP and GaP-rich alloys is due to transitions from shallow donors to the upper ⟨001⟩ minima at room temperature and below. The composition dependence of the threshold energy $h\nu_t$ is shown in Figure 11, where thre is some uncertainty as to the exact position of the donor level involved. The results obtained in the present study may have some uncertainty to this extent,

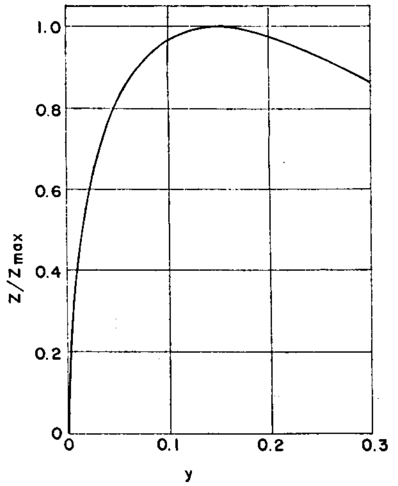

Fig. 12. A plot of $z/z_{\max}$ as a function of y obtained from the equation (5).

because E_t corresponds to E_0+E_1 in equation (3). The threshold energy depends to a small extent on the composition. In general, it seems to be caused by the linear dependency on the energy difference between X_1 and X_3 points with the specimen composition. The other possibility, however, is proposed as follows; when $E(X_1-X_3)$ is 0.30 eV in GaP, and then assumed that the energy difference between X_1 and X_3 point is independent on alloy compositions, a slight composition dependence of the threshold energy $h\nu_t$ should be caused by a change of donor ionization energy E_I. From Figure 11, the composition dependence of E_t may be represented by a straight line. When the donor ionization energy in *n*-GaP is taken to be 0.06 eV, the change of E_I with compositions is experimentally obtained to be 0.060–0.041 $(1-x)$, where x is the mole fraction of GaP in specimens. The donor ionization energy according to a simple hydrogen-like approximation is given by

$$E_I = -13.5\left(\frac{m^*}{m}\right)\frac{1}{\varepsilon^2}, \tag{8}$$

where ε is the dielectric constant. Then ε is to be 10.9 and 8.457 for GaAs and GaP, respectively. Therefore, the magnitude of the ionization energy for GaAs is deduced to be 0.036 eV. A slight dependence of E_t on composition could be practically explained in terms of an assumption of the linear relation of the dielectric constant with the composition of specimens.

The experimental data diverge at two points from the curve calculated from equation (3). First, the experimental absorption threshold, which is represented by $h\nu_t$ in Table 3, differs from the calculated one $h\nu_t$. Secondly, a reasonable fit for the higher temperature's data is difficult to be obtained with equation (3).

It seems that at temperatures well above room temperature most of the donors are ionized so that transitions from the lower to the upper ⟨001⟩ minima predominate with a consequent change in the magnitude and shape of the absorption.

One serious divergence between the experiment and the simple theory outlined above is that the threshold at low energies is not as sharp as expected. Near the absorption threshold the experimental results can be fitted by the empirical equation

$$\Delta\alpha \propto (h\nu - E_t')^x , \qquad (9)$$

where E_t' and x are empirical constants. A typical value obtained for x is 1.3. Several explanations for this absorption are possible: (1) In the group IV elements, the conduction band is degenerate at the zone boundary in the ⟨001⟩ direction, i.e. at the point X, while in III-V compounds the degeneracy is removed and two bands with symmetries X_1 and X_3 occur. Optical transitions between bands are allowed.[19] The absorption from such a transition should have a tail of exponential shape and vary exponentially with temperature. Experimentally it is found that at room temperature an exponential function is a poor approximation of the shape of the tail, but its transition may be possible at higher temperature.

(2) Phonon-assisted transitions will occur at lower energies than direct ones and cause a smearing-out of the sharp threshold. The phonon energies in GaP seem to be about a few hundredth of eV, which is less than the divergent energy.

(3) As to impurities, overlap between impurity atom wave functions is appreciable in our material and gives a spread of impurity ionization energies. Excited states of the impurity atoms are appreciably populated at the temperatures considered, and transitions from them will have a lower energy than transitions from the ground state. In this case, the absorption will be dependent on the impurity concentration n_I and vary exponentially with temperature. If the constant B in the 7th column of Table 3 does not change with composition, the term of Bn_I is only a function of n_I. The values of $1/a$ and $h\nu_{\max}$ are plotted as a function of Bn_I as shown in Figure 13, where $1/a$ is proportional to the donor ionization energy E_I

Table 3. Experimentally determined parameters of the additional absorption bands in n-GaP and n-GaP-rich side alloys.

Sample number	Alloy composition	E_t	$k_{\max}$	a	$Z_{\max}$	Bn_I	E_t'	x
P1	100	0.360 eV	3500 cm^{-1}	2.38×10^{-4}	11.7×10^4	5.3×10^5	0.285 eV	1.30
P2	100	0.360	5000	0.68	0.82	0.37	0.297	1.26
M15	71.0	0.351	3840	1.41	6.3	2.8	0.272	1.30
M12	50.0	0.337	3500	1.62	10.1	4.6	0.260	1.30
M11	48.0	0.334	3700	1.42	6.5	3.0	0.223	1.30

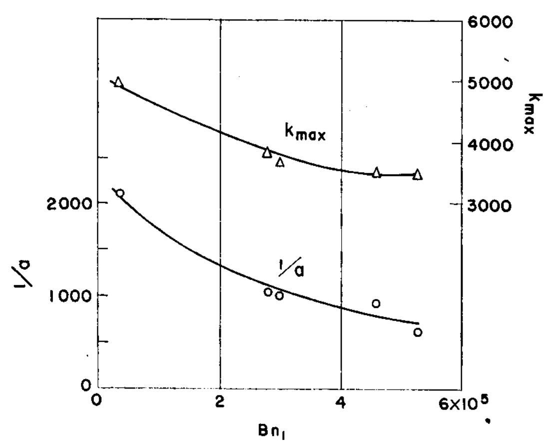

Fig. 13. Plots of $k_{\max}$ and $1/a$ va. Bn_I.

and increases with decreasing of the impurity concentration. The result may be interpreted from the existence of excited states of the impurity atoms.

3.2 Inter-conduction band transitions

The absorption band of n-GaAs or GaAs-rich alloy is rather broad and does not seem to have any remarkable peak as shown in Figures 3–4. In the first step of the analysis, the wave number dependence of z has been surveyed as similar to that of the previous section. Some results are shown in Figures 14 and 15 for n-GaAs and GaAs-rich specimens, respectively. Near the absorption threshold the experimental results can be fitted by the empirical equation

$$z = \Delta\alpha \cdot h\nu = A(h\nu - E_t)^x , \tag{10}$$

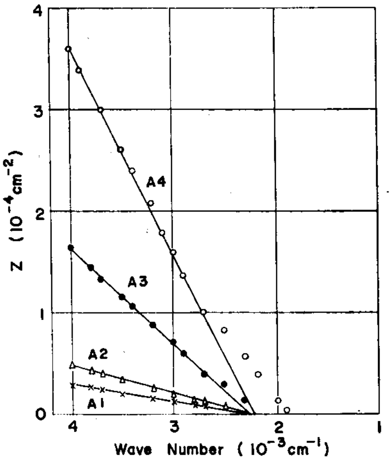

Fig. 14. Plots of z values as a function of wave numbers for specimens of A1, A2, A3 and A4.

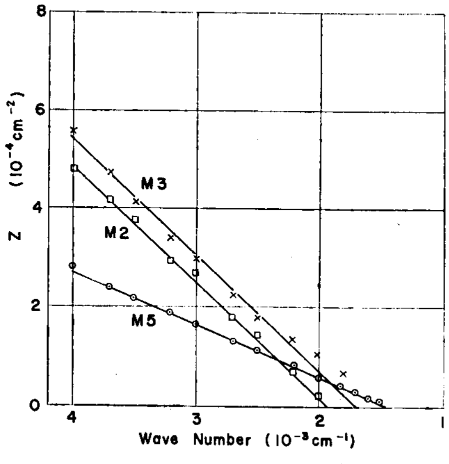

Fig. 15. Plots of z values as a function of wave numbers for specimens of M2, M3 and M5.

where E_t and x are empirical constants. A typical value found for x is 1.0 in n-GaAs and GaAs-rich specimens. The threshold energy for each specimen is reduced from a plot of z vs. $h\nu$. The threshold energy for n-GaAs with different carrier is nearly the same value at room temperature, but the lower carrier concentration specimens have a slightly higher energy than the higher one. The experimental absorption for the specimen A4 diverges from the equation (10) near the absorption threshold. The threshold energy for GaAs-rich specimens is observed to decrease to the lower energy side with increasing of the concentration of GaP component. These empirical threshold energies are shown in Table 4 and Figure 11.

Table 4. Empirical threshold energy due to inter-conduction band transition in n-GaAs and n-GaAs-rich alloys.

Sample number	Alloy composition	Empirical threshold energy (eV)	
		at 90°K	at 297°K
A1	0	0.407	0.298
A4	0	0.310	0.288
M1	4.0		0.270
M2	5.0		0.240
M3	12.0	0.248	0.210
M4	12.8		0.198
M5	14.7		0.181
M6	18.7		0.166
M7	22.0		0.148

In the case that an electron with wave vector $\boldsymbol{k}$, which is present near the lowest minimum of conduction band, makes a transition by the interaction with photons and crystal imperfections, into a state with wave vector $\boldsymbol{k}'$ in the conduction band of the subsidiary minimum which is present at the position different from the Γ-minimum, the transition probability should be calculated by use of the second order perturbation method. Haga and Kimura[9)] proposed that the absorption band calculated for the indirect type agrees well with the experimental one in n-GaAs at the points of the shape, the carrier concentration dependence and the temperature dependence as reported by Spitzer and Whelan. According to their model, the absorption is characterized as follows: (a) Acoustical phonon as the crystal imperfection contributes mainly for the absorption. Therefore, as the temperature decreases, the additional absorption band should change equally rapidly. (b) The absorption is proportional to carrier concentration. (c) The theoretical absorption coefficient contains an important adjustable parameter as $\Delta E_{10}=E(X_1-\Gamma_1)$. The additional absorption coefficient is represented by the integral equation

$$\Delta\alpha=\frac{C}{\theta}\int_u^\infty x^{1/2}\{x-(\Delta-\theta)\}^{1/2}dx\,, \tag{11}$$

where

$$x=\frac{\varepsilon}{kT}\,,\quad \Delta=\frac{\Delta E_{10}}{kT}\,,\quad \theta=\frac{h\nu}{kT}$$

and $h\nu$ is the photon energy, ΔE_{10} is the energy difference between X_1 and Γ_1 points in $\boldsymbol{k}$ space. The integral values as a function of ΔE_{10} are shown in Figure 16. E_{10} is reported to be 0.44 eV for GaAs.[9]

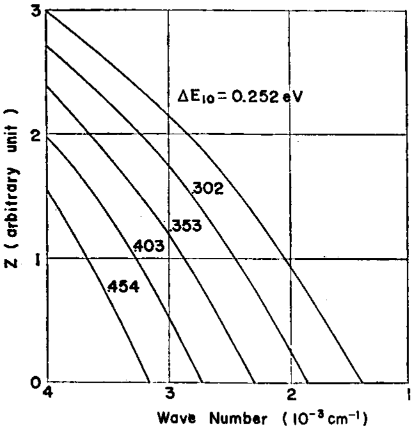

Fig. 16. The theoretical values of z as a function of wave numbers obtained by calculation.

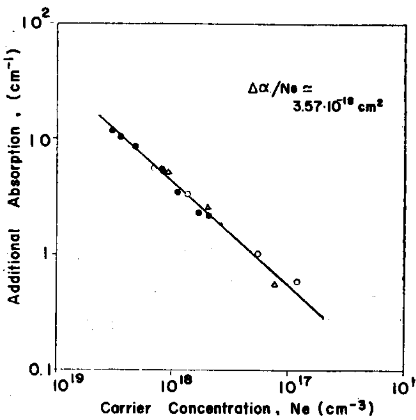

Fig. 17. The additional absorption coefficient for n-GaAs as a function of free carrier concentration at 3500 cm^{-1}.

The empirical threshold energy obtained previously from the equation (10) does not represent the true energy difference between Γ_1 and X_1 points as understood from the theoretical consideration. The change of the threshold energy with composition is shown in Figure 10, where the dotted curves express the difference between ⟨000⟩ and ⟨001⟩ minima and the cross over point occurs at 53% GaP according to Ehrenreich.[20] Then, according to the present experimental result, the threshold energy in GaAs-rich alloys has the dependence on composition x as $E_t=0.29-0.67\,x$ (eV). The empirical cross over point occurs at 43% GaP.

The other experimental interest in the treatment carried on by Haga and Kimura is discussed as follows; at a constant photon energy well above acoustical phonon energies, the additional absorption coefficient may be given by the equation,

$$\Delta\alpha \propto N_e(D-\Delta)\begin{Bmatrix} n_q \\ n_{q+1} \end{Bmatrix}, \tag{12}$$

assuming that the distribution function for conduction electrons is approximated by a Boltzman function, where N_e is the free carrier concentration, n_q is the acoustical phonon density and D is a constant. The absorption coefficients for n-GaAs samples at 3500 cm^{-1} are shown in Figure 17 as a function of free carrier concentration, where the absorption can be observed to change linearly with carrier concentration. The cross section due to this process is deduced to be 3.57×10^{-18} cm^2. Then, the cross sections were similarly determined for *n*-GaAs-rich specimens. The specimens of M5 and M6 are computed as the values of 9.9×10^{-18} and 14.0×10^{-18} cm^2, respectively. These cross sections for alloys are three or four times larger than for *n*-GaAs, as expected from the theory.

4. Conclusion

The present experimental results of the infrared absorption in the region from 1000 to 4000 cm^{-1} have given the following conclusions. (a) The absorption bands in *n*-GaP and GaP-rich alloys have been illustrated to occur mainly by a transition from a shallow donor level to the upper conduction band minimum. The reasonable fit for the absorption profile has been obtained with the equation (3), especially in the large wave number region. Near the absorption threshold the experimental values diverge from the equation (3). The fact might be interpreted in terms of the existence of excited states of the impurity atoms. The threshold energy depends to a small extent on the composition. The dependence could be illustrated in terms of the composition dependence of the donor ionization energy.

(b) The absorption in *n*-GaAs and GaAs-rich alloys arises from the bottom of the lowest conduction band to a subsidiary minimum. The absorption is represented with the equation (10). The dependence of threshold energy on composition x is found to be expressed as $E_t=0.29-0.67x$ (eV). The empirical cross over point occurs at 43 mol% GaP. At a constant photon energy well above acoustical phonon energies, it is concluded that the experimental absorption coefficient is proportional to the carrier concentration and the cross section for alloys are three or four times larger than for GaAs as expected from the theory.

5. Acknowledgments

The authors wish to express their appreciation to Mr. Shinichiro Akai of the Reserach Laboratory of Sumitomo Electric Industries, Ltd. for his valuable discussions through the course of this investigation. The works of Mr. Kanehiko Imanishi and Jun Inoue in sample preparation and measurements are greatly appreciated.

References

1) H. Ehrenreich; J. appl. Phys. Suppl. to 32 No. 10, (1961) 2155
2) M. Cardona, K.L. Shaklee and F.H. Pollak; Phys. Rev. **154** (1967) 696
3) M.L. Cohen and T.K. Bergstresser; Phys. Rev. **141** (1966) 789
4) F. Herman, R.L. Kortum, C.D. Kuglin and J.L. Shay; in II-IV Semiconducting Compounds, edited by D.G. Thomas (W.A. Benjamin, Inc. New York, 1967), p. 503
5) A.R. Hutson, A. Jayaraman and A.S. Coriell; Phys. Rev. **155** (1967) 786
6) J.M. Whelan and G.H. Wheatley; J. Phys. Chem. Solids **6** (1958) 169
7) L.W. Aukerman and R.K. Willardson; J. Appl. Phys. **31** (1960) 293
8) W.G. Spitzer and J.M. Whelan; Phys. Rev. **114** (1959) 59
9) E. Haga and H. Kimura; J. Phys. Soc. Japan **19** (1964) 1596
10) M. Shyam, J.W. Allen and G.L. Pearson; IEEE Trans. Electron Devices **13** (1966) 63
11) D. Madelung; Physics of III-V Compounds (John Wiley & Sons, Inc., New York, 1964), p. 531
12) I. Valslev; Phys. Rev. **173** (1968) 762
13) R. Zallen and W. Paul; Phys. Rev. **134** (1964) A1628
14) W.M. Becker, A.K. Ramdas and H.Y. Fan; J. appl. Phys. Suppl. to 32 No. 10, (1961) 2094
15) J.W. Allen and J.W. Hodby; Proc. Phys. Soc. **182** (1963) 315
16) K. Osamura and Y. Murakami; Abstract 2, Spring Meeting of Phys. Soc. of Japan, (1968) 147
17) B.O. Seraphin and H.E. Bennett in Semiconductors and Semimetals, edited by R.K. Willardson and A.C. Beer (Academic Press, New York and London, 1967) vol. 3, p. 499
18) H.W. Verleur and A.S. Barker, Jr.; Phys. Rev. **149** (1966) 715
19) G. Dresselhaus; Phys. Rev. **100** (1955) 582
20) H. Ehrenreich; Phys. Rev. **120** (1960) 1951
21) H.Y. Fan; Rep. Progr. Phys. **19** (1956) 107